

A Throughput-Based Adaptive MIMO-BICM Approach for Spatially-Correlated Channels

Matthew R. McKay^{*,†}, Iain B. Collings[†], Antonio Forenza[‡], and Robert W. Heath Jr.^{**}

^{*}Telecommunications Lab.,
Sch. of Elec. and Info. Engineering
University of Sydney, Australia

[†]Wireless Technologies Lab.,
ICT Centre, CSIRO, Australia

[‡]Freescale Semiconductor, Inc., Austin, TX, USA

^{**}Wireless Networking and Communications Group
Dept. of Electrical and Computer Engineering
The University of Texas at Austin, TX, USA

Abstract—This paper considers low complexity transmission for MIMO bit-interleaved coded modulation (BICM) in spatially-correlated Rayleigh channels. We consider both statistical beamforming (SB) and spatial-multiplexing with a zero-forcing (ZF) receiver. We derive tight closed-form bit error rate (BER) expressions based on a saddlepoint approximation. We then propose a practical adaptive algorithm which selects, based on the analytical results, the combination of code-rate, modulation format, and MIMO transmission scheme (SB or ZF) that maximizes throughput whilst maintaining a pre-defined BER.

Index Terms—BICM, MIMO, zero-forcing, spatial correlation

I. INTRODUCTION

There is a fundamental tradeoff between diversity and multiplexing in multiple-input multiple-output (MIMO) communication systems, and this is currently a topic of considerable research. In [1], an information-theoretic treatment was given for i.i.d. Rayleigh MIMO channels. In [2] and [3], practical approaches were designed to take advantage of this tradeoff, by adaptively switching between diversity and multiplexing transmission modes, depending on the channel quality. These uncoded schemes were shown to yield significant improvements over non-adaptive transmission in i.i.d. Rayleigh channels. A similar approach was also proposed in [4] for spatially-correlated channels, which adaptively selected a combination of a transmit-antenna subset and modulation format, based on the channel correlation scenario. This scheme was designed for channels with either transmit or receive correlation, but not both, and did not consider error-control coding.

In this paper we consider adaptive modulation and coding in MIMO channels with both transmit and receive correlation. The coding format we consider is bit-interleaved coded modulation (BICM), which is common in practical wireless systems (e.g. IEEE 802.11a WLANs, and proposed for IEEE 802.11n), and is ideally suited to adaptive transmission. Recently, non-adaptive BICM schemes have been applied to MIMO scenarios, and been shown to perform favorably with practical low complexity zero-forcing (ZF) receivers [5, 6],

This material is based in part upon work supported by the National Science Foundation under grant CCF-514194, the Office of Naval Research under grant number N00014-05-1-0169, and Freescale Semiconductor.

however it is expected that the performance will degrade in the presence of spatially-correlated channels. In this paper we propose to adapt between a BICM-ZF approach and a BICM statistical beamforming (SB) approach, depending on the channel correlation scenario.

We derive new bit error rate (BER) expressions for BICM-ZF in transmit and receive correlated channels. The results are based on the typical BICM assumption of ideal interleaving. This assumption is valid in channels with sufficient time variation or frequency selectivity. We make use of a saddlepoint approach, originally proposed in [7] for the single-input single-output (SISO) BICM case, and derive accurate closed-form expressions for the error probabilities.

Based on the analytical results, as well as corresponding BER results for BICM-SB¹, we identify and examine performance tradeoffs for the two MIMO transmission schemes. We then propose a practical adaptive BICM-mode and MIMO-transmission scheme selection algorithm, aimed at maximizing system throughput whilst maintaining a pre-defined acceptable BER. Our proposed approach is shown to yield significant throughput improvements in all channel correlation scenarios.

II. SYSTEM DESCRIPTION

A. Signal Model and Transmission Architecture

Consider a narrowband MIMO system with N_t and N_r transmit and receive antennas respectively. Throughout this paper we assume $N_t \leq N_r$, to facilitate low complexity BICM-ZF transmission (see below). For each channel use the received signal vector is given by

$$\mathbf{r} = \sqrt{\gamma} \mathbf{H} \mathbf{a} + \mathbf{n} \quad (1)$$

where $\mathbf{a} \in \mathcal{C}^{N_t \times 1}$ is the transmit signal vector satisfying the power constraint $E[\mathbf{a}^\dagger \mathbf{a}] = N_t$, and $\mathbf{n} \in \mathcal{C}^{N_r \times 1}$ is the noise vector $\sim \mathcal{CN}(\mathbf{0}_{N_r \times 1}, \mathbf{I}_{N_r})$. Also, $\mathbf{H} \in \mathcal{C}^{N_r \times N_t}$ is the spatially-correlated Rayleigh fading channel matrix, assumed to be known perfectly at the receiver, and γ is the average SNR per transmit antenna. The channel is modeled as follows

$$\mathbf{H} = \mathbf{R}^{\frac{1}{2}} \mathbf{H}_w \mathbf{S}^{\frac{1}{2}} \quad (2)$$

¹The BICM-SB BER analysis will be presented in an extended journal version of this paper [8].

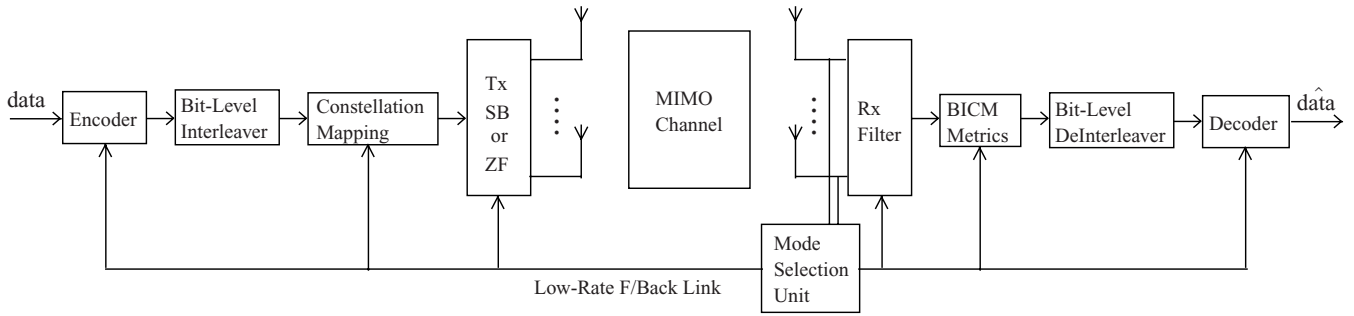


Fig. 1. MIMO-BICM system architecture.

where $\mathbf{H}_w \sim \mathcal{CN}(\mathbf{0}_{N_r \times N_t}, \mathbf{I}_{N_r} \otimes \mathbf{I}_{N_t})$, and $\mathbf{R} \in \mathcal{C}^{N_r \times N_r}$ and $\mathbf{S} \in \mathcal{C}^{N_t \times N_t}$ are the receive and transmit correlation matrices, with eigenvalue decompositions

$$\mathbf{R} = \mathbf{U}_r \mathbf{\Lambda}_r \mathbf{U}_r^\dagger \quad \mathbf{S} = \mathbf{U}_s \mathbf{\Lambda}_s \mathbf{U}_s^\dagger. \quad (3)$$

We assume that \mathbf{R} and \mathbf{S} are normalized Hermitian positive-definite matrices containing unit diagonal entries. Moreover, we assume that the eigenvector $\mathbf{u}_{s,\max}$ corresponding to the maximum eigenvalue of \mathbf{S} is known perfectly at the transmitter (this is to facilitate SB, see below). With this model, the average SNR per receive antenna is $N_t \gamma$.

Note that all analytical results presented in this paper apply equally to any particular correlation model. For the numerical studies we consider the exponential model (e.g. as in [9]),

$$\mathbf{R}_{i,j} = \rho_{rx}^{|i-j|} \quad \mathbf{S}_{i,j} = \rho_{tx}^{|i-j|} \quad (4)$$

where ρ_{rx} and ρ_{tx} are the receive and transmit spatial correlation coefficients between adjacent antennas. We choose this simple model (for the numerical studies) to illustrate clearly the impact of spatial correlation on the relative performance of the SB and ZF schemes.

The MIMO system architecture we consider is presented in Fig. 1. The encoder, interleaver (assumed ideal), and constellation mapper, form the BICM section of the transmitter. The BICM system operates according to one of a finite set of modes, with each mode comprising a particular combination of encoder rate and modulation format. The encoder rate R is varied by puncturing a mother binary convolutional encoder. The modulation formats are Gray-labeled 2^M -ary PSK/QAM constellations, denoted \mathcal{A} , of unit average energy. Mode selection is based on maximizing system throughput whilst maintaining a pre-defined acceptable BER.

Following modulation, the symbols are mapped to transmit signal vectors \mathbf{a} , according to the particular MIMO transmission scheme, as discussed in the following section.

B. Low Complexity MIMO Transmission Schemes

We now detail a SB scheme which we will show is suited to highly correlated channels or low SNRs, and a ZF scheme which will be shown to perform best in uncorrelated channels.

1) *Statistical Beamforming*: A single modulated symbol is transmitted on all the antennas, with an appropriate complex weighting, during each channel use. For a modulated symbol

$a \in \mathcal{A}$, the transmission vector \mathbf{a} is formed as follows

$$\mathbf{a} = \mathbf{u}_{s,\max} a. \quad (5)$$

The spectral efficiency of BICM-SB, in bits/s/Hz, is therefore

$$S_{\text{BICM-SB}} = RM. \quad (6)$$

2) *Zero-Forcing*: N_t modulated symbols are transmitted, one per antenna, during each channel use. The spectral efficiency of BICM-ZF, in bits/s/Hz, is therefore

$$S_{\text{BICM-ZF}} = N_t RM. \quad (7)$$

Clearly, for a given mode (combination of R and M), $S_{\text{BICM-ZF}}$ is larger than $S_{\text{BICM-SB}}$ by a factor of N_t .

C. Low Complexity MIMO-BICM Receivers

1) *Statistical Beamforming*: Maximum ratio combining (MRC) is applied to the receive signal vector to yield

$$\begin{aligned} z &= \mathbf{f}^\dagger \mathbf{r} = \sqrt{\gamma} \mathbf{f}^\dagger (\mathbf{H} \mathbf{u}_{s,\max} a + \mathbf{n}) \\ &= \sqrt{\gamma} \|\mathbf{f}\|^2 a + \underline{n} \end{aligned} \quad (8)$$

where $\mathbf{f} = \mathbf{H} \mathbf{u}_{s,\max}$ and $\underline{n} = \mathbf{f}^\dagger \mathbf{n} \sim \mathcal{CN}(0, \|\mathbf{f}\|^2)$. The BICM log-likelihood metrics for each of the bits corresponding to the symbol a are calculated from z , as in [8]. These are then deinterleaved and decoded using a Viterbi algorithm.

2) *Zero-Forcing*: The initial filtering step at the receiver is

$$\mathbf{z} = \mathbf{W} \mathbf{r} = \sqrt{\gamma} \mathbf{a} + \underline{\mathbf{n}} \quad (9)$$

where $\mathbf{W} = (\mathbf{H}^\dagger \mathbf{H})^{-1} \mathbf{H}^\dagger$ and $\underline{\mathbf{n}} = \mathbf{W} \mathbf{n}$. Clearly, the k^{th} element of \mathbf{z} corresponds to the output from a colored Gaussian noise channel, where the input is the k^{th} element of \mathbf{a} . For the k^{th} modulated symbol, a_k , the BICM log-likelihood metrics are then calculated for the corresponding bits, as shown in [5, 6], prior to deinterleaving and decoding.

III. PERFORMANCE ANALYSIS OF MIMO-BICM WITH ZERO-FORCING RECEIVERS

In this section we derive tight expressions for the BER of BICM-ZF. The corresponding results for BICM-SB will be presented in an extended journal version of this paper [8]. These results will provide the fundamental tools for establishing the selection criterion for our proposed adaptive MIMO-BICM algorithm in Section IV.

A. BER Union Bound

We consider linear, rate $R_c = k_c/n_c$, binary convolutional codes, for which a tight BER union bound is given by [10]

$$\text{BER} \leq \frac{1}{k_c} \sum_{d=d_{\text{free}}}^{\infty} W_I(d) f(d, \mu, \mathcal{A}, \gamma) \quad (10)$$

where $W_I(d)$ is the input weight of all error events at Hamming distance d , $f(\cdot)$ is the codeword pairwise error probability (C-PEP), μ is the labeling map, and d_{free} is the free Hamming distance.

B. Saddlepoint Approximation for the C-PEP

To simplify the C-PEP analysis we adopt the approach of [11] and force the BICM subchannels² to behave as binary-input output-symmetric (BIOS) channels by introducing a random bit-swapping variable u , which gives [10]

$$f(d, \mu, \mathcal{A}, \gamma) = \Pr \left(\sum_{i=1}^d \mathcal{L}_i > 0 \right) \quad (11)$$

assuming the all-zero codeword is transmitted, and where \mathcal{L}_i is the BICM log-likelihood metric for the i^{th} coded bit.

Since the C-PEP is the tail probability of a sum of i.i.d. random variables, a closed-form expression is obtained by applying a saddlepoint approximation [7, 12] to (11). This approximation is given by

$$f(d, \mu, \mathcal{A}, \gamma) \approx \frac{\mathcal{M}_{\mathcal{L}}(\hat{s})^d}{\sqrt{2\pi d \mathcal{K}_{\mathcal{L}}''(\hat{s}) \hat{s}}} \quad (12)$$

where $\mathcal{M}_{\mathcal{L}}(s) \triangleq E_{\mathcal{L}}[\exp(s\mathcal{L})]$ is the moment generating function (m.g.f.) of \mathcal{L} , $\mathcal{K}_{\mathcal{L}}''(\cdot)$ is the second derivative of the cumulant generating function (c.g.f.)

$$\mathcal{K}_{\mathcal{L}}(s) = \ln \mathcal{M}_{\mathcal{L}}(s) \quad (13)$$

and \hat{s} is the real value of s that minimizes $\mathcal{K}_{\mathcal{L}}(s)$ (and hence minimizes $\mathcal{M}_{\mathcal{L}}(s)$).

For BICM-ZF transmission, the m.g.f. is given by [13]

$$\mathcal{M}_{\mathcal{L}}(s) = E_{z, m, u, k, \mathbf{w}_k} \left[\exp \left(s \ln \frac{\sum_{\tilde{a} \in \mathcal{A}_u^m} \exp \left(-\frac{|z - \sqrt{\gamma} \tilde{a}|^2}{\|\mathbf{w}_k\|^2} \right)}{\sum_{\tilde{a} \in \mathcal{A}_u^m} \exp \left(-\frac{|z - \sqrt{\gamma} \tilde{a}|^2}{\|\mathbf{w}_k\|^2} \right)} \right) \right] \quad (14)$$

where \mathbf{w}_k is the k^{th} row of \mathbf{W} , and \mathcal{A}_u^m is the signal subset within \mathcal{A} with m^{th} bit equal to u . In [13] we previously presented a closed-form high SNR solution to (14) given by

$$\mathcal{M}_{\mathcal{L}}(s) = \frac{1}{N_t} \sum_{k=1}^{N_t} \sum_{i=1}^{|\mathcal{P}_M|} \mathcal{P}_{M,i} \tilde{\mathcal{I}}_{k, \mathcal{E}_{M,i}}(s) \quad (15)$$

where \mathcal{P}_M and \mathcal{E}_M are modulation specific sets, given in Table

²These are the equivalent channels between the transmitted binary codeword and the corresponding BICM bit metrics.

	\mathcal{P}_M	\mathcal{E}_M
BPSK	{1}	{4.0}
QPSK	{1}	{2.0}
16QAM	{3/4, 1/4}	{0.4, 1.6}
64QAM	{7/12, 1/4, 1/12, 1/12}	{0.0952, 0.3810, 0.8571, 1.5238}

TABLE I

\mathcal{P}_M AND \mathcal{E}_M FOR VARIOUS QAM/PSK CONSTELLATIONS (GRAY)

I, with i^{th} element $\mathcal{P}_{M,i}$ and $\mathcal{E}_{M,i}$ respectively, and

$$\tilde{\mathcal{I}}_{k, \mathcal{E}_{M,i}}(s) = \left| \mathbf{I}_{N_r} + \frac{\gamma \mathcal{E}_{M,i} s (1-s) \mathbf{\Lambda}_r}{[\mathbf{S}^{-1}]_{k,k}} \right|^{-1} \times \frac{\text{tr}_{N_t-1}(\mathbf{\Lambda}_r)}{\text{tr}_{N_t-1} \left(\mathbf{\Lambda}_r \left[\mathbf{I}_{N_r} + \frac{\gamma \mathcal{E}_{M,i} s (1-s) \mathbf{\Lambda}_r}{[\mathbf{S}^{-1}]_{k,k}} \right]^{-1} \right)} \quad (16)$$

where $[\cdot]_{k,k}$ denotes the k^{th} diagonal element, and $\text{tr}_{\ell}(\cdot)$ is the ℓ^{th} elementary symmetric function (e.s.f.) (see [14]).

The numerator of the saddlepoint approximation (12) for BICM-ZF is obtained by evaluating (15) and (16) at \hat{s} , which is easily found to be $\frac{1}{2}$. To evaluate the denominator of (12) we require $\mathcal{K}_{\mathcal{L}}''(\hat{s})$. Starting from (13) and (15), we have

$$\mathcal{K}_{\mathcal{L}}''(\hat{s}) = \frac{\mathcal{M}_{\mathcal{L}}''(\hat{s})}{\mathcal{M}_{\mathcal{L}}(\hat{s})} - \left(\frac{\mathcal{M}_{\mathcal{L}}'(\hat{s})}{\mathcal{M}_{\mathcal{L}}(\hat{s})} \right)^2 \quad (17)$$

where

$$\mathcal{M}_{\mathcal{L}}'(\hat{s}) = \frac{1}{N_t} \sum_{k=1}^{N_t} \sum_{i=1}^{|\mathcal{P}_M|} \mathcal{P}_{M,i} \tilde{\mathcal{I}}'_{k, \mathcal{E}_{M,i}}(\hat{s}) \quad (18)$$

$$\mathcal{M}_{\mathcal{L}}''(\hat{s}) = \frac{1}{N_t} \sum_{k=1}^{N_t} \sum_{i=1}^{|\mathcal{P}_M|} \mathcal{P}_{M,i} \tilde{\mathcal{I}}''_{k, \mathcal{E}_{M,i}}(\hat{s}). \quad (19)$$

To calculate $\tilde{\mathcal{I}}'(\cdot)$ and $\tilde{\mathcal{I}}''(\cdot)$ we manipulate $\tilde{\mathcal{I}}(\cdot)$ as follows. We first express the inverse in the denominator of (16) as³

$$[\mathbf{I}_{N_r} + K_{k,i}(s) \mathbf{\Lambda}_r]^{-1} = \text{diag} \left(\frac{1}{1 + K_{k,i}(s) \lambda_{r,q}} \right) \quad (20)$$

where $\lambda_{r,q}$ is the q^{th} eigenvalue of \mathbf{R} , and

$$K_{k,i}(s) \triangleq \frac{\gamma \mathcal{E}_{M,i} s (1-s)}{[\mathbf{S}^{-1}]_{k,k}}. \quad (21)$$

We also write the determinant in (16) as

$$|\mathbf{I}_{N_r} + K_{k,i}(s) \mathbf{\Lambda}_r| = \prod_{j=1}^{N_r} (1 + K_{k,i}(s) \lambda_{r,j}). \quad (22)$$

Using (20) and (22) we obtain

$$\tilde{\mathcal{I}}_{k, \mathcal{E}_{M,i}}(s) = \frac{\text{tr}_{N_t-1}(\mathbf{\Lambda}_r)}{\text{tr}_{N_t-1} \left(\text{diag} \left(\frac{\lambda_{r,q}}{1 + K_{k,i}(s) \lambda_{r,q}} \right) \right) \prod_{j=1}^{N_r} (1 + K_{k,i}(s) \lambda_{r,j})} \quad (23)$$

Now using properties of e.s.f.s, we can express the denomi-

³Here we introduce a compact notation to represent the diagonal matrix in terms of the q^{th} diagonal element.

$$f(d, \mu, \mathcal{A}, \gamma) \approx \frac{1}{2N_t^d \sqrt{\pi d}} \frac{\left(\sum_{k=1}^{N_t} \sum_{i=1}^{|\mathcal{P}_M|} \mathcal{P}_{M,i} \left(1 + \sum_{\ell=1}^{N_r - N_t + 1} \left(\frac{\gamma \mathcal{E}_{M,i}}{4[\mathbf{S}^{-1}]_{kk}} \right)^\ell C_\ell \right)^{-1} \right)^{d+\frac{1}{2}}}{\sqrt{\sum_{k=1}^{N_t} \sum_{i=1}^{|\mathcal{P}_M|} \mathcal{P}_{M,i} \frac{\sum_{\ell=1}^{N_r - N_t + 1} \ell \left(\frac{\gamma \mathcal{E}_{M,i}}{4[\mathbf{S}^{-1}]_{kk}} \right)^\ell C_\ell}{\left(1 + \sum_{\ell=1}^{N_r - N_t + 1} \left(\frac{\gamma \mathcal{E}_{M,i}}{4[\mathbf{S}^{-1}]_{kk}} \right)^\ell C_\ell \right)^2}}}} \quad (27)$$

nator as a polynomial in s , which leads to

$$\tilde{\mathcal{I}}_{k, \mathcal{E}_{M,i}}(s) = \left(1 + \sum_{\ell=1}^{N_r - N_t + 1} K_{k,i}(s)^\ell C_\ell \right)^{-1} \quad (24)$$

where

$$C_\ell \triangleq \sum_{\{\alpha\}} \left(\prod_{j=1}^{N_t-1} \lambda_{r, \alpha_j} \right) \text{tr}_\ell(\text{diag}(\lambda_{r, \beta_q})) \quad (25)$$

for $\ell = 1, \dots, N_r - N_t + 1$, where the sum is over all ordered $\alpha = \{\alpha_1, \dots, \alpha_{N_t-1}\} \subseteq \{1, \dots, N_r\}$, and $\{\beta_1, \dots, \beta_{N_r - N_t + 1}\} = \{1, \dots, N_r\} \setminus \alpha$.

Now, using (24), we perform some tedious algebra to evaluate $\tilde{\mathcal{I}}'_{k, \mathcal{E}_{M,i}}(\hat{s})$ and $\tilde{\mathcal{I}}''_{k, \mathcal{E}_{M,i}}(\hat{s})$ as follows

$$\tilde{\mathcal{I}}'_{k, \mathcal{E}_{M,i}}(\hat{s}) = 0$$

$$\tilde{\mathcal{I}}''_{k, \mathcal{E}_{M,i}}(\hat{s}) = 8\tilde{\mathcal{I}}_{k, \mathcal{E}_{M,i}}(\hat{s})^2 \left(\sum_{\ell=1}^{N_r - N_t + 1} \ell C_\ell \left(\frac{\gamma \mathcal{E}_{M,i}}{4[\mathbf{S}^{-1}]_{kk}} \right)^\ell \right). \quad (26)$$

We now substitute (26) into (18) and (19), simplify the result, and then use (17) and (12) to give the final closed-form C-PEP saddlepoint approximation in (27) at the top of the page.

1) *Special Case: $N_t = 2, N_r = 2$:* For 2×2 systems, (27) reduces to the following simple expression

$$f(d, \mu, \mathcal{A}, \gamma) \approx \frac{\left(\sum_{i=1}^{|\mathcal{P}_M|} \mathcal{P}_{M,i} \left(1 + \frac{\gamma \mathcal{E}_{M,i} |\mathbf{R}| |\mathbf{S}|}{4} \right)^{-1} \right)^{d+\frac{1}{2}}}{2\sqrt{\pi d} \sum_{i=1}^{|\mathcal{P}_M|} \mathcal{P}_{M,i} \frac{\frac{\gamma \mathcal{E}_{M,i} |\mathbf{R}| |\mathbf{S}|}{4}}{\left(1 + \frac{\gamma \mathcal{E}_{M,i} |\mathbf{R}| |\mathbf{S}|}{4} \right)^2}} \quad (28)$$

C. Simplified C-PEP at High SNR

In the high SNR regime, we note that the summations over ℓ in (27) are dominated by the terms corresponding to $\ell = N_r - N_t + 1$, and obtain

$$f(d, \mu, \mathcal{A}, \gamma) \approx \left(\frac{\gamma}{4} \right)^{-(N_r - N_t + 1)d} \frac{\text{tr}_{N_t-1}(\mathbf{A}_r)^d}{2N_t^d \sqrt{\pi d} \binom{N_r}{N_t-1}^d |\mathbf{R}|^d} \times \left(\sum_{k=1}^{N_t} \sum_{i=1}^{|\mathcal{P}_M|} \mathcal{P}_{M,i} \left(\frac{\mathcal{E}_{M,i}}{[\mathbf{S}^{-1}]_{kk}} \right)^{-(N_r - N_t + 1)d} \right)^d \quad (29)$$

which is clearly much simpler than (27).

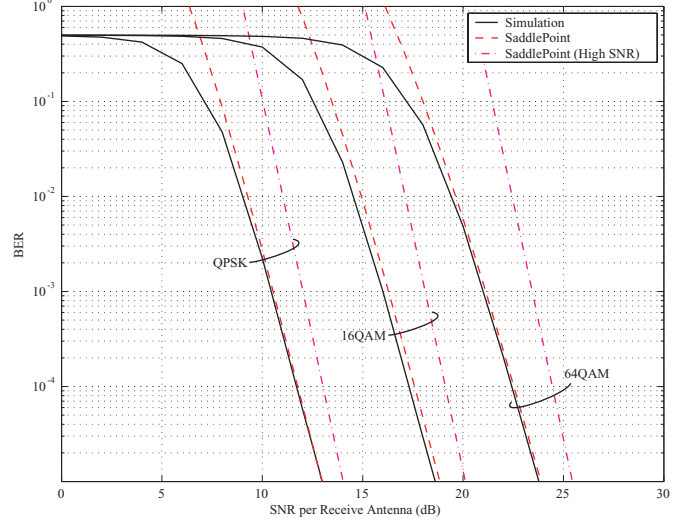


Fig. 2. Simulated and analytical BER of 2×2 BICM-ZF employing the optimal $\frac{1}{2}$ rate code ($d_{\text{free}} = 10$). An exponential correlation model is used, with correlation coefficient 0.5 at both the transmitter and receiver.

1) *Special Case: $N_t = 2, N_r = 2$:* In this case, (29) reduces to the extremely simple expression

$$f(d, \mu, \mathcal{A}, \gamma) \approx \frac{1}{2\sqrt{\pi d}} \left(\frac{\gamma |\mathbf{R}| |\mathbf{S}|}{4} \left(\sum_{i=1}^{|\mathcal{P}_M|} \frac{\mathcal{P}_{M,i}}{\mathcal{E}_{M,i}} \right)^{-1} \right)^{-d} \quad (30)$$

D. BER Performance Results

Fig. 2 compares the analytical BICM-ZF BER expressions with Monte-Carlo simulation results. Results are shown for the optimal $1/2$ -rate 64-state code ($d_{\text{free}} = 10$) with ideal interleaving, and the correlation model (4) with $\rho_{\text{tx}} = \rho_{\text{rx}} = 0.5$. The ‘saddlepoint’ curves were obtained by substituting the C-PEP expression (28) into (10), and are clearly tight for low to moderate BERs. The ‘saddlepoint (high SNR)’ curves were obtained from (30). We see that these curves tighten as the BER is reduced, and are within 2 dB of the simulated curves for BERs below 10^{-5} .

IV. ADAPTIVE MIMO-BICM TRANSMISSION

Before presenting the details of the adaptive strategy, we first investigate the relative performance of BICM-SB and BICM-ZF in various correlation scenarios.

Fig. 3 considers 2×2 fully-interleaved systems, and shows tight BER curves based on the C-PEP expression (28) for

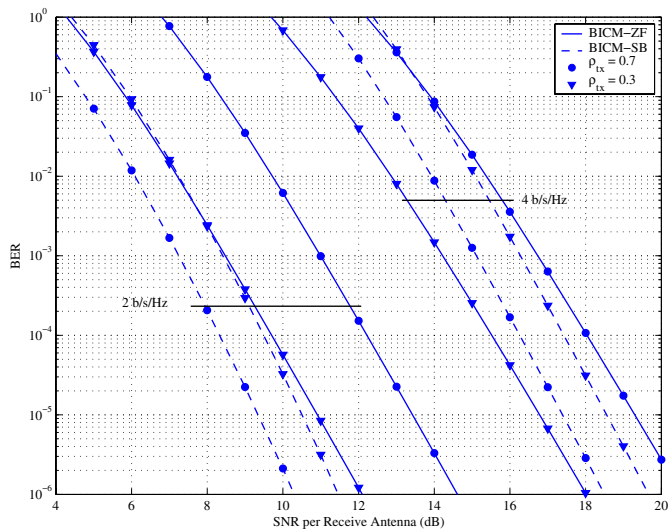


Fig. 3. BER curves based on the tight C-PEP expressions for 2×2 BICM-ZF and BICM-SB. Two exponential correlated scenarios, with $\rho_{rx} = 0.1$, $\rho_{tx} = 0.3$, and $\rho_{rx} = 0.1$, $\rho_{tx} = 0.7$.

BICM-ZF, and for BICM-SB see [8]. For the 2 bits/s/Hz case, BICM-SB operates with a 1/2 rate code and 16QAM, and BICM-ZF operates with a 1/2 rate code and QPSK. For the 4 bits/s/Hz case, BICM-SB operates with a 2/3 rate code (obtained by puncturing the 1/2 rate code above, as outlined in [15]) and 64QAM, whereas BICM-ZF operates with the 1/2 rate code and 16QAM.

As expected, we see that BICM-ZF degrades with increasing transmit correlation. In contrast, the BER of BICM-SB *improves* with increasing transmit correlation. This improvement is due to more energy being focused in the direction of the SB vector $\mathbf{u}_{s,max}$, yielding an SNR gain. The relative performance is of course the important factor in designing a switching scheme, and this is highly influenced by the correlation and the spectral efficiency. The figure shows that for 2 bits/s/Hz, BICM-SB outperforms BICM-ZF in both correlation scenarios. However at 4 bits/s/Hz, BICM-SB is best for $\rho_{tx} = 0.7$, and BICM-ZF is best for $\rho_{tx} = 0.3$.

A. Analytical BICM Mode and MIMO Transmission Scheme Selection Algorithm

Clearly there are significant benefits to be gained from switching between BICM-ZF and BICM-SB depending on the channel correlation scenario and the SNR. We now propose a low complexity practical switching algorithm that jointly selects the best combination of MIMO transmission scheme (i.e. SB or ZF) and BICM mode (code-rate and modulation format) to maximize the system throughput whilst satisfying a predefined target BER. The proposed selection algorithm is based on the closed-form BER results.

The throughput ν is calculated for a given BICM mode and MIMO transmission scheme using

$$\nu = S(1 - \text{BER}) \quad (31)$$

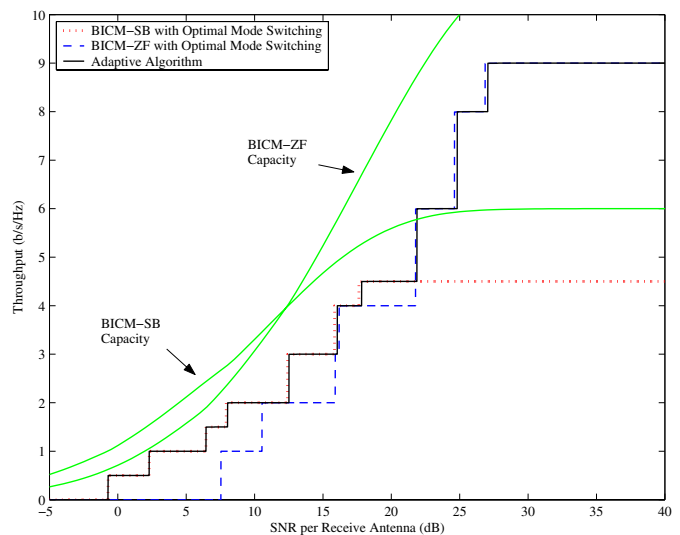


Fig. 4. Throughput achieved by adaptive algorithm for 2×2 antennas, target BER 10^{-3} , and exponential correlation parameters $\rho_{rx} = \rho_{tx} = 0.5$. Selection based on tight C-PEP expressions. Throughputs with optimal mode selection and LLC envelopes also given.

where S is the spectral efficiency. For a given mode, the spectral efficiencies are calculated for the SB and ZF transmission schemes according to (6) and (7) respectively.

In general terms, we follow a standard adaptive procedure whereby the receiver first estimates channel parameters, then calculates which mode will yield the highest throughput, and then conveys that information to the transmitter via a reliable low-rate feedback link. A key novelty of our scheme is that we perform switching based on the channel spatial correlation matrix eigenvalues, and that we switch between the MIMO transmission schemes (SB and ZF) as well as coding and modulation formats. It is the new closed-form BER expressions of the previous sections which make this possible.

B. Throughput Performance Results

In this section, we consider 2×2 systems, and employ the eight BICM modes defined by the IEEE 802.11a standard in [15]. Note, however, that our algorithm applies equally to any antenna configuration, and for any set of modes comprising Gray-labeled modulation formats.

Fig. 4 shows throughput results for a target BER of 10^{-3} , and for correlated channels with $\rho_{rx} = \rho_{tx} = 0.5$. The figure shows the throughputs obtained by BICM-SB and BICM-ZF with optimal mode switching, where the switching points are calculated based on the actual simulated BER curves. For comparison, optimal BICM link-level capacity (LLC) envelope curves (derived in [8]), are also shown. The solid line in the figure corresponds to our proposed adaptive selection algorithm, where the switching points are based on the tight C-PEP expressions (28) for BICM-ZF, and for BICM-SB see [8]. Clearly our approach achieves near-optimal throughputs for all SNR. As expected, BICM-SB is selected for low SNRs, and BICM-ZF is selected for high SNRs.

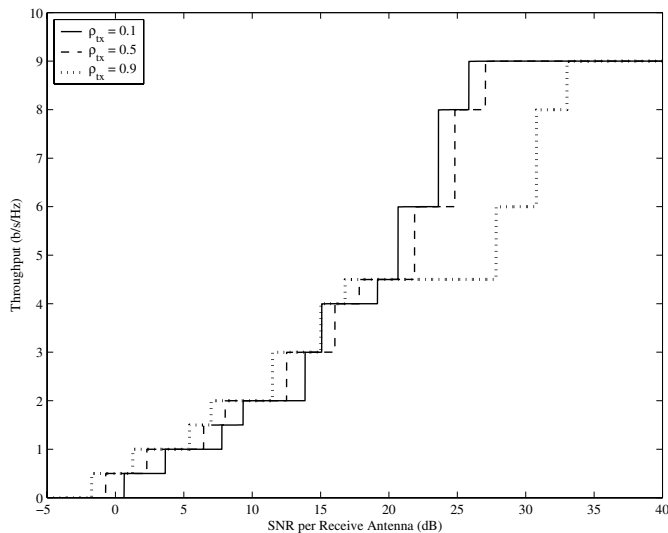


Fig. 5. Throughputs achieved by the proposed adaptive algorithm for a 2×2 system with target BER 10^{-3} , in different exponential correlated channel scenarios, with $\rho_{rx} = 0.5$, and ρ_{tx} values of 0.1, 0.5 and 0.9. Selection is based on the tight C-PEP expressions.

Fig. 5 shows the throughputs of the proposed adaptive algorithm in various transmit correlation scenarios. For SNRs below 20 dB, the throughputs improve with increasing transmit correlation, since BICM-SB was selected by the adaptive algorithm in this low SNR regime. Conversely, for SNRs above 20 dB, the adaptive algorithm selected BICM-ZF, and hence the throughput degrades with increasing transmit correlation.

V. CONCLUSION

This paper presented a practical adaptive algorithm for MIMO-BICM transmission in spatially-correlated Rayleigh channels, and showed that significant throughput gains could be achieved by optimizing the choice of code-rate, modulation format, and MIMO transmission scheme. Tight closed-form BER expressions were derived, and were used to determine switching criteria in the proposed adaptive algorithm.

REFERENCES

- [1] L. Zheng and D. N. C. Tse, "Diversity and multiplexing: A fundamental tradeoff in multiple-antenna channels," *IEEE Trans. Inform. Theory*, vol. 49, no. 5, pp. 1073–1096, May 2003.
- [2] R. W. Heath Jr. and A. Paulraj, "Switching between multiplexing and diversity based on constellation distance," in *Proc. Allerton Conf. on Comm. Control. and Comp.*, Monticello, IL, Sept. 2000.
- [3] R. W. Heath Jr. and D. J. Love, "Multi-mode antenna selection for spatial multiplexing systems with linear receivers," in *Proc. Allerton Conf. on Comm. Control and Comp.*, Monticello, IL, Oct. 2003.
- [4] R. Narasimhan, "Spatial multiplexing with transmit antenna and constellation selection for correlated MIMO fading channels," *IEEE Trans. Signal Processing*, vol. 51, no. 11, pp. 2829–2838, Nov. 2003.
- [5] M. R. G. Butler and I. B. Collings, "A zero-forcing approximate log-likelihood receiver for MIMO bit-interleaved coded modulation," *IEEE Commun. Lett.*, vol. 8, no. 2, pp. 105–107, Feb. 2004.
- [6] M. R. McKay and I. B. Collings, "Capacity and performance of MIMO-BICM with zero forcing receivers," *IEEE Trans. Commun.*, vol. 53, no. 1, pp. 74–83, Jan. 2005.
- [7] A. Martinez, A. Guillén i Fàbregas, and G. Caire, "New simple evaluation of the error probability of bit-interleaved coded modulation using the saddlepoint approximation," in *Proc. IEEE Int. Symp. on Info. Theory and Appl. (ISITA)*, Parma, Italy, Oct. 2004.

- [8] M. R. McKay, I. B. Collings, A. Forenza, and R. W. Heath Jr., "Adaptive coded-MIMO in spatially-correlated channels based on closed-form BER expressions," *IEEE Trans. Veh. Technol.*, 2006, submitted.
- [9] M. Kiessling and J. Speidel, "Mutual information of MIMO channels in correlated Rayleigh fading environments - a general solution," in *Proc. IEEE Int. Conf. on Comm. (ICC)*, Paris, France, Jun 2004, pp. 814–818.
- [10] A. J. Viterbi and J. K. Omura, *Principles of Digital Communication and Coding*. New York: McGraw-Hill, 1979.
- [11] G. Caire, G. Taricco, and E. Biglieri, "Bit-interleaved coded modulation," *IEEE Trans. Inf. Theory*, vol. 44, no. 3, pp. 927–946, May 1998.
- [12] R. Gallager, *Information Theory and Reliable Communication*. John Wiley and Sons, 1968.
- [13] M. R. McKay and I. B. Collings, "Error performance of MIMO-BICM with zero-forcing receivers in spatially-correlated Rayleigh channels," *IEEE Trans. Wireless Commun.*, 2005, to appear.
- [14] A. W. Marshall and I. Olkin, *Inequalities: Theory of Majorization and Its Applications*. New York: Academic, 1979.
- [15] IEEE 802.11, "Supplement to IEEE standard for telecommunications and information exchange between systems - LAN and MAN specific requirements," IEEE Std 802.11a-1999, September 1999.